Supporting Information

Metal−Metal Redox Synergy in Selective B−H Activation of *ortho*-Carborane-9,12-dithiolate

*Xiaolei Zhang, Zhiwen Zhou, Hong Yan**

State Key Laboratory of Coordination Chemistry, School of Chemistry and Chemical Engineering, Nanjing University, Nanjing, Jiangsu 210093, China

Table of Contents

1. Genaral procedure

$[Cp^*RhCl_2]_2$, ferrocenium hexafluorophosphate and $Rh(PPh_3)_3Cl$ are commercial available. 9,12-dimercapto-1,2-carborane ([9,12-2SH-1,2-$C_2B_{10}H_{10}$]) was prepared according to literature method.[S1] The other reagents were purchased from commercial vendors and used without further purification unless otherwise noted. All manipulations were carried out using standard Schlenk or glovebox techniques under an atmosphere of argon unless otherwise noted. Solvents were dried and deoxygenated prior to use. Hexanes, THF, toluene and petroleum ether were refluxed and distilled over sodium/benzophenone under nitrogen. Dichloromethane and chloroform were distilled over CaH_2 under nitrogen.

Spectroscopic measurements. ^1H, ^{11}B, ^{31}P, and ^{13}C spectra were collected on Bruker DRX 400, 500 and 600 MHz NMR spectrometers. ^1H NMR spectra were referenced to the solvent peaks used. ^{13}C NMR chemical shifts were reported in ppm referenced to TMS (δ = 0 ppm). ^{11}B spectra were given with respect to external $Et_2O{\cdot}BF_3$ ($\delta^{11}B$ = 0 ppm). ^{31}P spectra were referenced to external 85% phosphoric acid (δ = 0 ppm). The mass spectra were recorded on Finnigan MAT TSQ7000 for ESI-MS. The IR spectra were recorded on a Bruker Vector 22 spectrophotometer with KBr pellets in the region of 4000–400 cm^{-1}. Elemental analysis was performed in an elementar vario EL III elemental analyzer.

High resolution mass spectra (HRMS) measurements. Mass spectrometry has been reported to be a very effective method to identify boron-containing compounds, especially for carborane derivatives.[S2] All of the new complexes in this work have

been characterized by electrospray ionization (ESI) method, which were recorded on Finnigan MAT TSQ7000 and Agilent-G6540. Complexes **4, 5, 10** and the intermediates **I, II, IV** in the reaction of complex **4** and water have been characterized by high resolution mass spectra which were carried out on LTQ-Orbitrap XL mass spectrometer (ThermoFisher, Bremen, Germany). The instrument was tuned to facilitate the ionization process and achieve the highest sensitivity and calibrated according to the manufacturer's instructions both in positive and negative ion detection modes using the manufacturer's calibration solution (consisting of caffeine, the tetrapeptide MRFA and Ultramark). The mass spectrometric conditions were initially optimized by direct infusion of solution of complexes **4** or **5** (well characterized by X-ray, NMR, ESI-MS and element analysis in this study) at ca. 1.0 mg/L into the ionization source using a carrier solution of MeOH (Merck) with or without 0.1% (v/v) formic acid. The solution of complex **4** and water was injected directly by a syringe at 5 μL/min. The positive ion mode was primarily used and the electrospray voltage, heated capillary temperature and voltage, tube lens voltage, sheath gas flow rate and auxiliary gas flow rate were varied to maximize the ion transmission. The parameters were set as below: ion spray voltage 3.5 kV, capillary voltage 37 V, tube lens 120 V, capillary temperature 300 ^{o}C, sheath gas flow 0 (arbitrary units), auxiliary gas flow 0 (a.u.). Since most of the complexes contain *nido*-carborane unit, the loss of H_2 molecule was observed under the applied ionization conditions. Note that loss of H_2 for carboranes or polyhedron boranes during mass measurements is common. [S2a,b]

X-ray Crystallography. X-ray diffraction data were collected on a Bruker SMART Apex II CCD diffractometer by means of graphitemonochromated Mo Kα (λ = 0.71073) radiation at 291 K. During collection of the intensity data, no significant decay was observed. The intensities were corrected for Lorentz polarization effects and empirical absorption by using the SADABS program.[S3] The structures were solved by direct methods with the SHELXL-97 program.[S4] All non-hydrogen atoms were found from difference Fourier synthesis. The bound rhodium hydrides were also found from difference Fourier synthesis. The other hydrogen atoms were placed at geometrically calculated positions and refined using a riding model. All calculations were performed by using the Bruker SMART program. Crystallographic data (CCDC No. 996712–996721) of **2**, **3**, **4**, **5**, **7**, **8**, **9**, **11, 12** and **13** are included in Table S2.

2. Experimental section

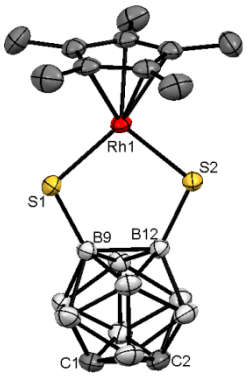

Fig. S1 Molecular structure of complex **2.** Selected bond distances [Å] and bond angles [º]: C1–C2 1.630(4), B9–S1 1.838(3) B12–S2 1.843(3) Rh1–S1 2.2920(7), Rh1–S2 2.3079(7), S1−Rh1−S2 96.27(2).

Preparation of compound 2 [Cp*Rh(9,12-$S_2C_2B_{10}H_{10}$)]. 9,12-dithiol-1,2-*o*-carborane (82 mg, 0.4 mmol) was dissolved in CH_2Cl_2 (30 mL) and Et_3N (0.15 mL,

1.0 mmol) was added to the solution, the resulting mixture was stirred for 15 min at room temperature. Then $[Cp^*RhCl_2]_2$ (122 mg, 0.2 mmol) was added to the mixture. The solution turned green instantly. After 1h, the solvent was removed *in vacuo* and the residue was chromatographed on silica gel by CH_2Cl_2 to give **2** (160 mg, 90% based on **1**). Single crystals suitable for X-ray analysis were obtained by slow concentration of a CH_2Cl_2 solution. Color: green. m.p.: 255−256 ºC. ^{1}H NMR ($CDCl_3$): δ = 1.79 (s, 15H, C**H**$_3$), 1.70−2.81 (br, 8H, cage−B**H**), 2.96 (s, 2H, cage−C**H**); ^{11}B {^{1}H} NMR ($CDCl_3$): δ = 18.7 (2B, **B**−S), −4.5 (3B), −11.4 (3B), −13.0 (2B); ^{13}C NMR ($CDCl_3$): δ = 10.3 (Cp*−**C**H$_3$), 36.7 (cage−**C**), 94.4 (d, J_{Rh-C} = 6 Hz, Cp*). ESI-MS (positive ion mode) *m/z*: 468.50 ([M+Na]$^+$, 100%). IR(KBr): ν (cm^{-1}) 2557 (B−H), 2567 (B−H). Anal. Calcd for $C_{12}H_{25}B_{10}S_2Rh$: C, 33.43; H, 5.67. Found: C, 33.15; H, 5.79.

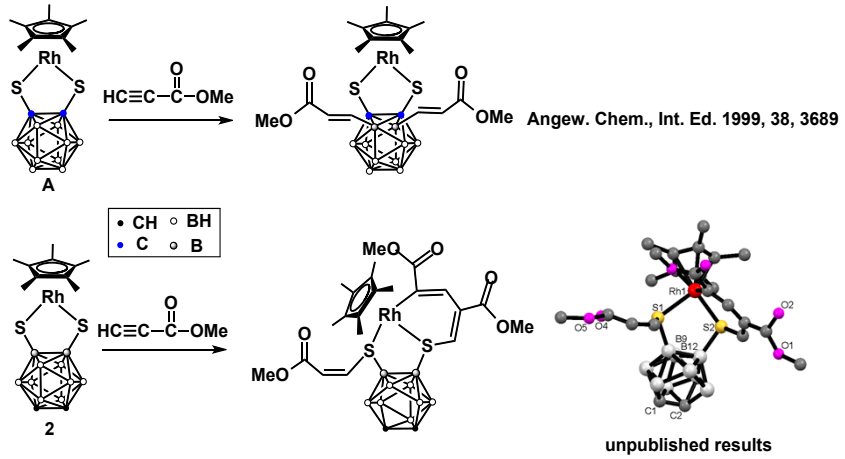

Scheme S1. Compared reactivity of 16e complexes **A** and **2** toward HC≡CC(O)OMe. The reactivity of **A** led to B(3)/(6) functionalized species which was published in 1999 whereas the reactivity of **2** was restricted at Rh−S bonds and no B(8)/(10) functionalized species were observed.

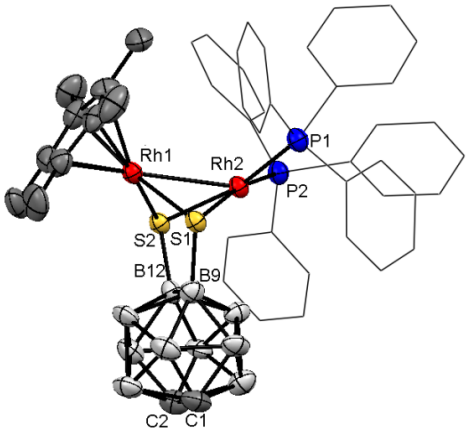

Fig. S2 Molecular structure of complex **3** (only cationic part is shown). Selected bond distances [Å] and bond angles [º]: (There are two independent molecules in the asymmetric unit) C1−C2 1.645(6), 1.605(6), B–S 1.877(5) to 1.903(5), Rh−S 2.3314(10) to 2.4503(10), Rh2−P 2.2842(11) to 2.3281(10), Rh1−Rh2 2.7678(4), 2.7648(5).

Preparation of complex 3 [Cp*Rh$_2$(PPh$_3$)$_2$(9,12-S$_2$C$_2$B$_{10}$H$_{10}$)PF$_6$]. NH_4PF_6 (33 mg, 0.2 mmol) and $Rh(PPh_3)_3Cl$ (185 mg, 0.2 mmol) were added to a CH_2Cl_2 (20 mL) solution of compound **2** (76 mg, 0.2 mmol). After 6 hours at room temperature, the solvent was removed *in vacuo* and the residue was chromatographed on silica gel by CH_2Cl_2 to give **3** (205 mg, 88%). Single crystals suitable for X-ray analysis were obtained by slow diffusion of hexanes into a CH_2Cl_2 solution of **3**. Color: green. m.p.: 204 ºC (dec). ^{1}H NMR ($CDCl_3$): δ = 1.63 (s, 15H, Cp*−C**H**$_3$), 1.6−3.1 (br, 8H, cage−B**H**), 3.86 (s, 2H, cage−C**H**), 7.16−7.29 (30H, Ph); ^{11}B {^{1}H} NMR ($CDCl_3$): δ = 15.0 (2B, **B**−S), 2.3 (1B), −0.9 (3B), −16.1 (4B); ^{31}P {^{1}H} NMR ($CDCl_3$): 33.2 (d, $^1J_{Rh-P}$ = 171 Hz, **P**Ph$_3$), −144.6 (sep, **P**F$_6$); ^{13}C {^{1}H} NMR ($CDCl_3$): δ = 10.6 (Cp*−**C**H$_3$), 48.2 (cage−**C**), 96.9 (d, $^1J_{Rh-C}$ = 7.5 Hz, Cp*), 127.8 (Ph−**C**H), 129.8 (Ph−**C**H), 134.2 (Ph−**C**H), 134.7 (Ph−**C**). ESI-MS (positive ion mode) *m/z*: 1072.00

([M]$^+$, 100%), ESI-MS (negative ion mode) *m/z*: 145.00 (PF_6^-, 100%), IR(KBr): ν (cm^{-1}) 2596 (B−H). Anal. Calcd for $C_{48}H_{55}B_{10}P_3S_2Rh_2F_6$: C, 47.38; H, 4.56. Found: C, 47.01; H, 4.42.

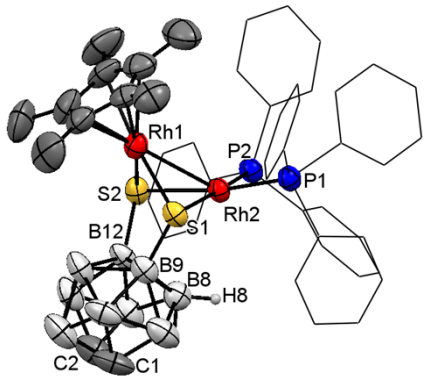

Fig. S3 Molecular structure of complex **4.** Selected bond distances [Å] and bond angles [º]: C1−C2 1.579(10), B9–S1 1.879(6), B12–S2 1.881(6), Rh−S 2.3255(13) to 2.4103(13), Rh1−Rh2 2.7466(6), Rh2−P1 2.3041(13), Rh2−P2 2.2979(13).

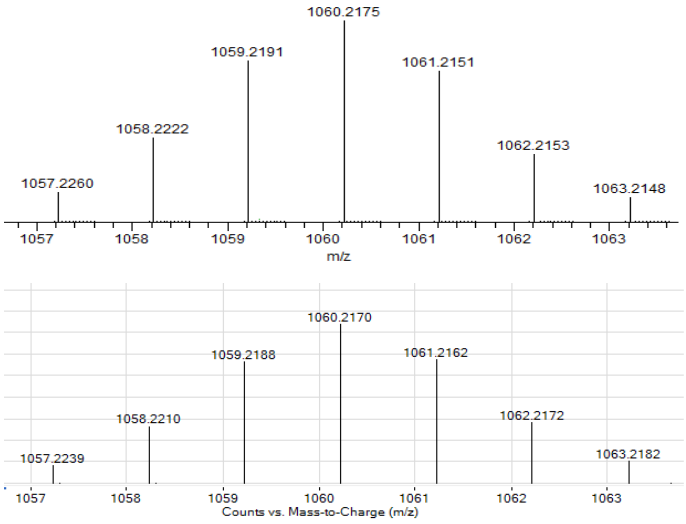

Fig. S4 ESI-HRMS of complex **4**. Measured $[M+H^+-H_2]^+$ = 1060.2170 for **4** (down) and calculated ($[M+H^+-H_2]^+$ = 1060.2175 for M = $C_{48}H_{55}B_9P_2S_2Rh_2$) (up).

Preparation of complex 4 [$Cp^*Rh_2(PPh_3)_2(S_2C_2B_9H_{10})$]. A CH_3OH solution of complex **3** (243 mg, 0.2 mmol) was added 1.0 equiv of CsF (33 mg, 0.2 mmol) and

the resulting mixture was stirred for 8h at 60 ºC. Then solvent was removed *in vacuo* and the residue was chromatographed on silica gel by hexanes/toluene (1 : 1) to give **4** (179 mg, 80%). Single crystals suitable for X-ray analysis were obtained by slow diffusion of hexanes into a toluene solution of **4**. Color: green. m.p.: 237 ºC (dec). ^{1}H NMR (C_6D_6): δ = −0.76 (br q, 1H, B−**H**−B), 1.68 (s, 15H, C**H**$_3$), 1.4−3.0 (br, 7H, cage−B**H**), 1.80 (s, 2H, cage−C**H**), 7.11 − 7.35 (30H, Ph); ^{11}B {^{1}H} NMR (C_6D_6): δ = 3.2 (2B, **B**−S), −10.2 (2B), −16.3 (2B), −23.3 (2B), −28.6 (1B); ^{31}P {^{1}H} NMR (C_6D_6): 35.6 (d, J_{Rh-P} = 173 Hz). ^{13}C {^{1}H} NMR (C_6D_6): δ = 11.3 (Cp*−**C**H$_3$), 39.2 (cage−**C**), 96.2 (d, $^{1}J_{Rh-C}$ = 7.5 Hz, Cp*), 128.1 (Ph−**C**H), 129.7 (Ph−**C**H), 135.2 (Ph−**C**H), 136.4 (Ph−**C**). ESI-HRMS (positive ion mode) *m/z*: 1060.2170 ([M+H$^+$−H$_2$]$^+$, 100%), IR(KBr): ν (cm^{-1}) 2540 (B−H). Anal. Calcd for $C_{48}H_{55}B_9P_2S_2Rh_2$: C, 54.33; H, 5.22. Found: C, 53.99; H, 5.31.

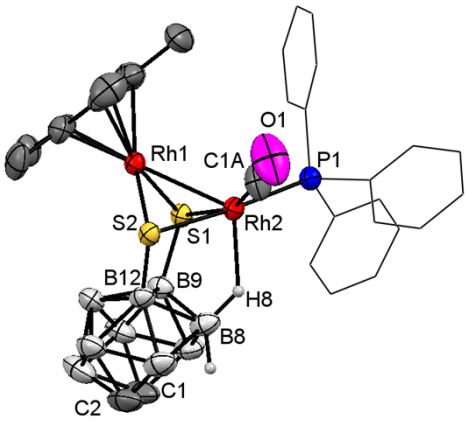

Fig. S5 Molecular structure of complex **5**. Selected bond distances [Å] and bond angles [º]: C1−C2 1.566(8), B9–S1 1.897(5), B12–S2 1.883(5), Rh−S 2.3340(10) to 2.4299(10), Rh1−Rh2 2.7272(5), Rh2−P1 2.2961(11), Rh2−C1A 1.817(5), C1A−O1 1.140(6), Rh2−H8 2.0746, B8−H8 1.1893.

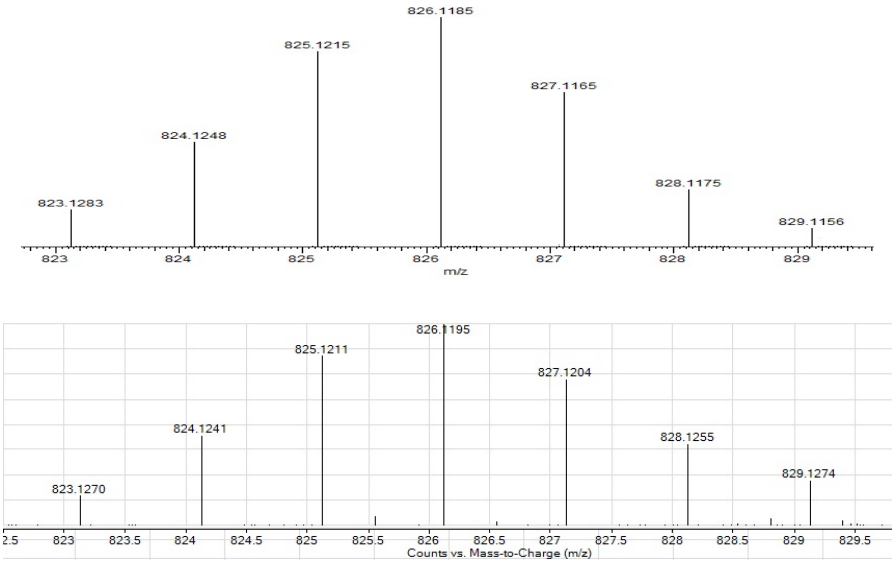

Fig. S6 ESI-HRMS of complex **5**. Measured $[M+H^+-H_2]^+$ = 826.1195 for **5** (down) and calculated ($[M+H^+-H_2]^+$ = 826.1185 for M = $C_{31}H_{40}B_9PS_2Rh_2O$) (up).

Preparation of complex 5 [Cp*Rh$_2$(PPh$_3$)(CO)(S$_2$C$_2$B$_9$H$_{10}$)]. Complex **4** (212 mg, 0.2 mmol) was dissolved in toluene (10 mL), and carbon monoxide was bubbled into the solution for 30 min. Then the solvent was removed *in vacuo* and the resulting residue was washed with hexanes (10 mL) to give **5** (161 mg, 99%). Color: blue. m.p.: 188 ºC (dec). ^{1}H NMR (C_6D_6): δ = −1.21 (br q, 1H, Rh−**H**−B), −1.07 (br q, 1H, B−**H**−B), 1.35 (s, 15H, C**H**$_3$), 1.7−3.3 (br, 6H, cage−B**H**), 1.98 (s, 1H, cage−C**H**), 2.10 (s, 1H, cage−C**H**), 6.99−7.11 (15H, Ph); ^{11}B {^{1}H} NMR (C_6D_6): δ = 4.3 (1B, **B**−S), 0.4 (1B, **B**−S), −10.6 (1B), −15.1 (1B), −17.1 (1B), −19.9 (1B), −20.9 (1B), −23.0 (1B), −34.8 (1B, Rh−H−B); ^{31}P {^{1}H} NMR (C_6D_6): 36.0 (d, J_{Rh-P} = 150 Hz). ^{13}C {^{1}H} NMR (C_6D_6): δ = 10.5 (s, Cp*−**C**H$_3$), 37.0 (cage−**C**), 41.7 (cage−**C**), 96.6 (d, J_{Rh-C} = 7.5 Hz, Cp*), 129.0 (Ph−**C**H), 130.7 (Ph−**C**H), 134.5 (Ph−**C**H), 134.7 (Ph−**C**), 189.3 (dd, $^1J_{Rh-C}$ = 78 Hz, $^2J_{P-C}$ = 10.5 Hz, **C**O). ESI-HRMS (positive ion mode) *m/z*: 826.1195 ($[M+H^+-H_2]^+$, 100%), IR(KBr): ν (cm^{-1}) 2520 (B−H), 1980

(C≡O). Anal. Calcd for $C_{31}H_{40}B_9PS_2Rh_2O$: C, 45.03; H, 4.88. Found: C, 44.65; H, 4.75.

Preparation of complex 6 [Cp*Rh$_2$(PPh$_3$)$_2$Cl(S$_2$C$_2$B$_9$H$_9$)]. Complex **4** (212 mg, 0.2 mmol) was dissolved in CH_2Cl_2 (20 mL), then ferrocenium hexafluorophosphate ($FcPF_6$) (66.2 mg, 0.2 mmol) was added to the solution and the mixture was allowed to stir at room temperature for 30 min. The solvent was removed *in vacuo* and the residue was chromatographed on silica gel by hexanes/toluene (2 : 1) to give **6** (138 mg, 83%). Color: yellow. m.p.: 165 ºC (dec). ^{1}H NMR (C_6D_6): δ = −1.04 (br q, 1H, B−**H**−B), 1.41 (s, 15H, C**H**$_3$), 1.8−3.0 (br, 6H, cage−B**H**), 2.01 (s, 2H, cage−C**H**), 6.96−7.04 (30H, Ph); ^{11}B {^{1}H} NMR (C_6D_6): δ = 5.7 (2B, **B**−S), 0.6 (2B), −17.6 (2B), −27.2 (2B), −39.7 (Rh−**B**); ^{31}P {^{1}H} NMR (C_6D_6): 20.6 (d, J_{Rh-P} = 125 Hz). ^{13}C {^{1}H} NMR (C_6D_6): δ = 10.1 (Cp*−CH_3), 38.7 (cage−C), 95.9 (d, J_{Rh-C} = 7.5 Hz, Cp*), 128.8 (Ph−**C**H), 131.1 (Ph−**C**H), 134.5 (Ph−**C**), 135.3 (Ph−**C**H). ESI-MS (positive ion mode) *m/z*: 1094.00 ([M+H$^+$−H$_2$]$^+$, 100%), IR(KBr): ν (cm^{-1}) 2543 (B−H). Anal. Calcd for $C_{48}H_{54}B_9P_2S_2ClRh_2$: C, 52.62; H, 4.97. Found: C, 52.48; H, 5.16.

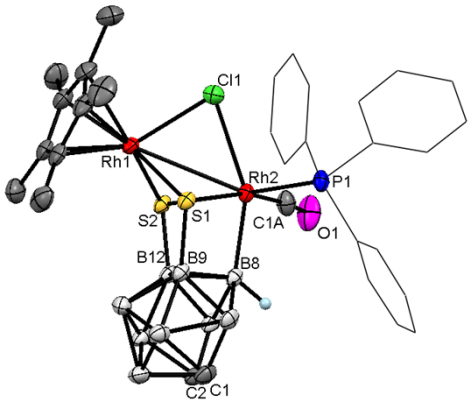

Fig. S7 Molecular structure of complex **7**. Solvent molecules are omitted for clarity. Selected bond distances [Å] and bond angles [º]: C1−C2 1.580(6), B9−S1 1.880(5),

B12−S2 1.886(5), Rh−S 2.3839(10) to 2.4344(12), Rh1−Rh2 3.1566(5), B8−Rh2 2.112(5), Rh1−Cl1 2.4723(11), Rh2−P1 2.3034(12), Rh2−C1A 1.862(4), C1A−O1 1.139(5), Rh2−Cl1 2.5836(11), Cl1−Rh2−Rh1 49.81(3), Cl1−Rh1−Rh2 52.96(3), Rh1−Cl1−Rh2 77.23(3).

Preparation of complex 7 [Cp*Rh_2(PPh_3)Cl(CO)($S_2C_2B_9H_9$)]. Complex **5** (165 mg, 0.2 mmol) was dissolved in CH_2Cl_2 (20 mL), ferrocenium hexafluorophosphate ($FcPF_6$) (66.2 mg, 0.2 mmol) was added into the solution and the mixture was allowed to stir at room temperature for 30 min. The solvent was removed *in vacuo* and the residue was chromatographed on silica gel by hexanes/toluene (3 : 1) to give **7** (153 mg, 88%). Single crystals suitable for X-ray analysis were obtained by cooling a cyclohexane solution of **7** at −20 ºC. Color: yellow. m.p.: 169 ºC (dec). ^{1}H NMR (C_6D_6): δ = −1.03 (br q, 1H, B−**H**−B), 1.36 (s, 15H, C**H**$_3$), 1.8−3.0 (br, 6H, cage−B**H**), 1.83 (s, 1H, cage−C**H**), 1.92 (s, 1H, cage−C**H**), 6.96−7.04 (15H, Ph); ^{11}B {^{1}H} NMR (C_6D_6): δ = 6.1 (1B, **B**−S), 5.7 (1B, **B**−S), 0.8 (1B), −13.4 (1B), −16.5 (2B), −28.0 (2B), −36.8 (1B, Rh−**B**); ^{31}P {^{1}H} NMR (C_6D_6): 32.9 (d, J_{Rh-P} = 125 Hz). ^{13}C {^{1}H} NMR (C_6D_6): δ = 9.4 (Cp*−**C**H$_3$), 38.6 (cage−**C**), 38.9 (cage−**C**), 95.9 (d, J_{Rh-C} = 7.5 Hz, Cp*), 128.8 (Ph−**C**H), 131.1 (Ph−**C**H), 134.5 (Ph−**C**), 135.3 (Ph−**C**H), 186.7 (dd, $^1J_{Rh-C}$ = 78 Hz, $^2J_{P-C}$ = 10.5 Hz, **C**O). ESI-MS (positive ion mode) *m/z*: 860.17 ([M+H$^+$−H$_2$]$^+$, 100%), IR(KBr): ν (cm^{-1}) 2523 (B−H), 1968 (C≡O). Anal. Calcd for $C_{31}H_{39}B_9PS_2Rh_2OCl$: C, 43.23; H, 4.56. Found: C, 42.91; H, 4.71.

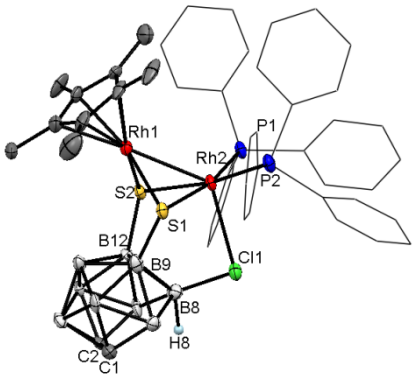

Fig. S8 Molecular structure of complex **8**. Solvent moleculars are omitted for clarity. Selected bond distances [Å] and bond angles [º]: C1−C2 1.570(5), Rh−S 2.3327(9) to 2.4227(8), Rh1−Rh2 2.7389(4), B8−Cl1 1.843(4), Rh2−Cl1 2.6789(10), Rh2−P2 2.3144(9), Rh2−P1 2.3285(9).

Preparation of complex 8 [$Cp^*Rh_2(PPh_3)_2(S_2C_2B_9H_9Cl)$]. Compound **6** (109 mg, 0.1 mmol) was added to a solution of CH_2Cl_2 (10 mL). After stirring for 8 h at room temperature, the solvent was removed in *vacuo* and the residue was chromatographed on neutral alumina gel by hexanes and CH_2Cl_2 v/v = (3:1) to give gray complex **8** (93 mg, 85%). Single crystals suitable for X-ray analysis were obtained by slow diffusion of hexanes into a CH_2Cl_2 solution of **8** under argon atmosphere. Color: brown. m.p.: 207 ºC. ^{1}H NMR (C_6D_6): δ = −3.68 (br q, 1H, B−**H**−B), 1.59 (s, 15H, C**H**$_3$), 1.6−3.1 (br, 6H, cage−B**H**), 2.07 (s, 2H, cage−C**H**), 7.07 − 7.22 (30H, Ph); ^{11}B {^{1}H} NMR (C_6D_6): δ = 5.0 (3B, **B**−S and **B**−Cl resonance overlapped), −7.6 (1B), −10.7 (1B), −19.3 (2B), −22.8 (2B); ^{31}P {^{1}H} NMR (C_6D_6): 29.6 (d, J_{Rh-P} = 158 Hz); ^{13}C {^{1}H} NMR (C_6D_6): δ = 10.7 (Cp^*−**C**H$_3$), 38.8 (cage−**C**), 104.2 (d, J_{Rh-C} = 7.5 Hz, Cp^*), 129.4 (Ph−**C**H), 131.9 (Ph−**C**H), 135.5 (Ph−**C**H), 135.9 (Ph−**C**). ESI-MS (positive ion mode) *m/z*: 1094.00 ([M+H$^+$−H$_2$]$^+$, 100%). IR(KBr): ν (cm^{-1}) 2574 (B−H). Anal. Calcd for $C_{48}H_{54}B_9P_2S_2ClRh_2$: C, 52.62; H,

4.97. Found: C, 52.28; H, 5.10.

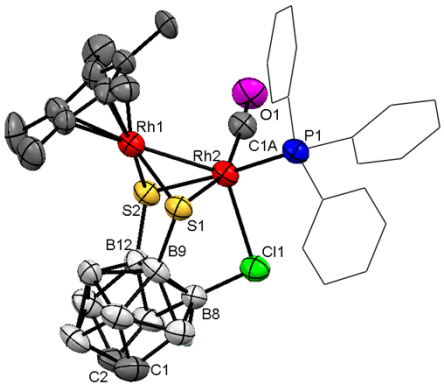

Fig. S9 Molecular structure of complex **9**. Selected bond distances [Å] and bond angles [º]: C1−C2 1.575(8), B9−S1 1.912(5), B12−S2 1.909(6), Rh−S 2.3568(14) to 2.4219(14), Rh1−Rh2 2.6885(6), Rh2−C1A 1.841(6) C1A−O1 1.147(6), B8−Cl1 1.807(6), Rh2−P1 2.3033(14), Rh2−Cl1 2.6976(14), B8−Cl1−Rh2 93.67(19).

Preparation of complex 9 [Cp*Rh$_2$(PPh$_3$)(CO)(S$_2$C$_2$B$_9$H$_9$Cl)]. A similar procedure to the preparation of **8** was conduct by replacing complex **6** by **7** to give complex **9** (68 mg, 81%). Single crystals suitable for X-ray analysis were obtained by slow diffusion of hexanes into a CH_2Cl_2 solution of **9**. Color: brown. m.p.: 234 ºC (dec.). ^{1}H NMR (C_6D_6): δ = −1.73 (br q, 1H, B−**H**−B), 1.71 (s, 15H, C**H**$_3$), 1.8−3.1 (br, 6H, cage−B**H**), 1.90 (s, 1H, cage−C**H**), 1.96 (s, 1H, cage−C**H**), 6.99 − 7.07 (15H, Ph); ^{11}B {^{1}H} NMR (C_6D_6): δ = 5.2 (1B, **B**−Cl), 4.5 (1B, **B**−S), 3.2 (1B, **B**−S), −6.2 (1B), −9.7 (1B), −10.3 (1B), −12.9 (1B), −19.1 (1B), −22.3 (1B); ^{31}P {^{1}H} NMR (C_6D_6): 35.2 (d, J_{Rh-P} = 137 Hz). ^{13}C {^{1}H} NMR (C_6D_6): δ = 10.9 (Cp*−**C**H$_3$), 38.2 (cage−**C**), 39.0 (cage−**C**), 104.4 (d, J_{Rh-C} = 7.5 Hz, Cp*), 129.3 (Ph−**C**H), 131.8 (Ph−**C**H), 135.3 (Ph−**C**H), 135.8 (Ph−**C**), 187.5 (dd, $^1J_{Rh-C}$ = 78 Hz, $^2J_{P-C}$ = 10.5 Hz, **C**O). ESI-MS (positive ion mode) *m/z*: 860.17 ([M+H$^+$−H$_2$]$^+$, 100%). IR (KBr): ν

(cm^{-1}) 2530 (B−H), 1980 (C≡O). Anal. Calcd for $C_{31}H_{39}B_9PS_2Rh_2OCl$: C, 43.23; H, 4.56. Found: C, 42.98; H, 4.43.

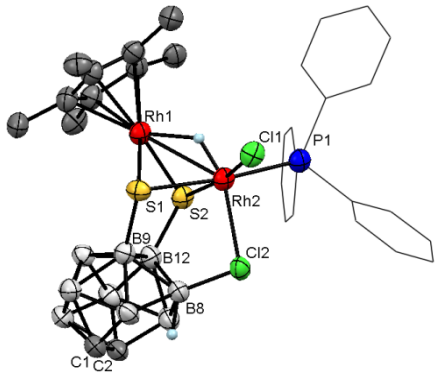

Fig. S10 Molecular structure of complex **11**. Solvent molecules are omitted for clarity. Selected bond distances [Å] and bond angles [º]: C1−C2 1.554(4), B9−S1 1.896(3), B12−S2 1.885(3), Rh−S 2.3422(8) to 2.4378(8), Rh1−Rh2 2.6946(4), B8−Cl2 1.858(3), Rh2−Cl1 2.3729(8), Rh2−Cl2 2.4784(8), Rh−H 1.2921, 1.7324, Rh1−H−Rh2 125.35, Rh2−Cl2−B8 96.63(10).

Preparation of complex 11 [Cp*Rh$_2$HClPPh$_3$(S$_2$C$_2$B$_9$H$_9$Cl)]. A $CHCl_3$ solution of complex **4** (242 mg, 0.2 mmol) was heated at 60 ºC for 6 h. The reaction mixture turned from dark green to red. The solvent was removed *in vacuo* and the residue was washed with hexanes. Extraction of the residue with CH_2Cl_2 (10 mL) followed by filtration gave a red solution that was concentrated to 2 mL, hexanes was diffused into this solution to afford red crystals of compound **11** (113 mg, 65%). Color: red. m.p.: 193 ºC (dec). ^{1}H NMR ($CDCl_3$): δ = −18.81 (dt, $^1J_{Rh-H}$ = 20 Hz, $^2J_{P-H}$ = 10 Hz, 1H, Rh−**H**−Rh), −1.69 (br q, 1H, B−**H**−B), 1.89 (s, 15H, C**H**$_3$), 1.4−3.0 (br, 6H, cage−B**H**), 2.06 (s, 1H, cage−C**H**), 2.11 (s, 1H, cage−C**H**), 7.37−7.65 (15H, Ph); ^{11}B {^{1}H} NMR ($CDCl_3$): δ = 5.4 (1B, **B**−Cl), 3.4 (2B, **B**−S), −0.7 (1B), −5.0 (1B), −6.7 (1B), −10.0 (1B), −20.2 (1B), −24.0 (1B); ^{31}P {^{1}H} NMR

($CDCl_3$): 31.5 (d, J_{Rh-P} = 125 Hz). ^{13}C {^1H} NMR ($CDCl_3$): δ = 10.7 (Cp*−CH_3), 42.3 (cage−C), 44.3 (cage−C), 100.3 (d, J_{Rh-C} = 7.5 Hz, Cp*), 128.1 (Ph−**C**H), 130.7 (Ph−**C**H), 134.2 (Ph−**C**), 134.7 (Ph−**C**H). ESI-MS (positive ion mode) *m/z*: 870.50 ($[M+H]^+$, 100%), IR(KBr): ν (cm^{-1}) 2538 (B−H), 1975 (Rh−H). Anal. Calcd for $C_{30}H_{40}B_9PS_2Cl_2Rh_2$: C, 41.42; H, 4.64. Found: C, 41.04; H, 4.75.

Conversion from complex 11 to 9. To a toluene solution of complex **11** (86.8 mg, 0.1 mmol) was added 1 equiv of CsF (20 mg, 0.1 mmol) and the mixture was heated for 6h at 60 ºC under a CO balloon. Complex **9** was isolated (72.4 mg, 63%).

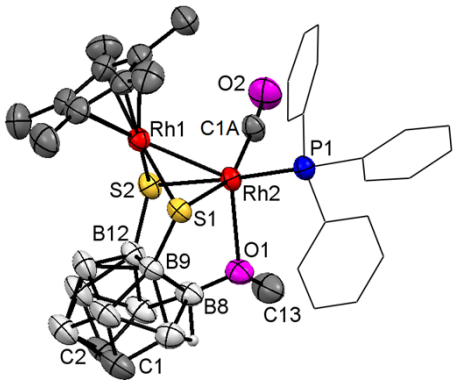

Fig. S11 Molecular structure of complex **12**. Selected bond distances [Å] and bond angles [º]: C1−C2 1.561(11), B9−S1 1.886(7), B12−S2 1.882(7), Rh−S 2.3382(16) to 2.4270(14), Rh1−Rh2 2.7023(7), Rh2−C1A 1.827(6) C1A−O2 1.117(7), B8−O1 1.424(8), Rh2−P1 2.2831(16), Rh2−O1 2.4704(4), B8−O1−Rh2 106.0(4).

Preparation of complex 12 [Cp*Rh_2(CO)PPh_3($S_2C_2B_9H_9OCH_3$)]. Compound **4** (168 mg, 0.2 mmol) was dissolved in 20 mL dry CH_3OH and heated at 60 ºC for 24 h. Then carbon monoxide was bubbled into the solution for 15 min. The solvent was removed *in vacuo* and the residue was chromatographed on silica gel by hexanes and CH_2Cl_2 (2 : 1) to give complex **12** (142 mg, 82 %). Single crystals suitable for single

crystal analysis were obtained by slow diffusion of hexanes into a CH_2Cl_2 solution of **12**. Color: violet. m.p.: 189 ºC. (dec). ^{1}H NMR ($CDCl_3$): δ = −1.84 (br q, 1H, B−**H**−B), 1.67 (s, 15H, C**H**$_3$), 1.5−3.1 (br, 6H, cage−B**H**), 2.08 (s, 2H, cage−C**H**), 3.51 (s, 3H, O−C**H**$_3$), 7.39−7.55 (m, 15H, Ph); ^{11}B {^{1}H} NMR ($CDCl_3$): δ = 5.8 (1B, **B**−O), −2.9 (2B, **B**−S), −7.0 (1B), −9.4 (1B), −18.6 (1B), −22.8 (1B), −24.9 (2B); ^{31}P {^{1}H} NMR ($CDCl_3$): 37.7 (d, J_{Rh-P} = 139 Hz), ^{13}C NMR ($CDCl_3$): δ = 10.3 (Cp*−**C**H$_3$), 42.0 (cage−**C**), 62.6 (O**C**H$_3$), 95.7 (d, J_{Rh-C} = 7.5 Hz, Cp*), 128.3 (Ph−**C**H), 130.3 (Ph−**C**H), 133.9 (Ph−**C**H), 134.8 (Ph−**C**), 188.3 (dd, $^1J_{Rh-C}$ = 78 Hz, $^2J_{P-C}$ = 10.5 Hz, **C**O). ESI-MS (positive ion mode) *m/z*: 857.14 ([M+H$^+$−H$_2$]$^+$, 100%), IR(KBr): ν (cm^{-1}) 2542 (B−H), 1973 (C≡O). Anal. Calcd for $C_{31}H_{42}B_9N_2PS_2Rh_2O$: C, 43.45; H, 4.94. Found: C, 43.23; H, 5.11.

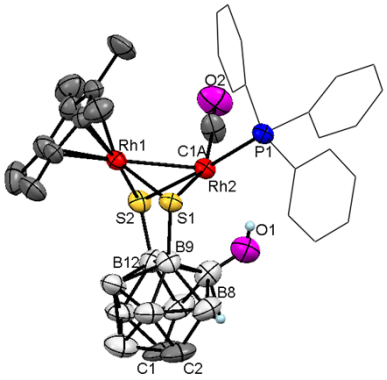

Fig. S12 Molecular structure of complex **13**. Selected bond distances [Å] and bond angles [º]: C1−C2 1.561(8), B9−S1 1.884(5), B12−S2 1.879(6), Rh−S 2.3293(12) to 2.4233(12), Rh1−Rh2 2.7124(5), Rh2−C1A 1.823(5) C1A−O2 1.135(6), B8−O1 1.411(7), O1−H1A 0.8200, Rh2−P1 2.2887(11).

Preparation of complex 13 [Cp*Rh$_2$(CO)PPh$_3$(S$_2$C$_2$B$_9$H$_9$OH)]. Compound **4** (168 mg, 0.2 mmol) and 0.1 mL of water (25 equiv.) were added to 20 mL toluene and the mixture was heated at 60 ºC for 15 h. After that carbon monoxide was

bubbled into the solution for 15 min. The solvent was removed in *vacuo* and the residue was chromatographed on silica gel by hexanes and CH_2Cl_2 (3:2) to give blue complex **13** (148 mg, 89%). Single crystals suitable for X-ray analysis were obtained by slow diffusion of hexanes into a CH_2Cl_2 solution of **13**. Color: blue. m.p.: 196 ºC (dec). ^{1}H NMR ($CDCl_3$): δ = −1.91 (br q, 1H, B−**H**−B), 1.66 (s, 15H, C**H**$_3$), 1.4−2.9 (br, 6H, cage−B**H**), 2.09 (s, 2H, cage−C**H**), 7.39 − 7.55 (15H, Ph); ^{11}B {^{1}H} NMR ($CDCl_3$): δ = 4.4 (1B, **B**−O), 3.1 (2B, **B**−S), −6.2 (1B), −8.1 (1B), −11.3 (1B), −13.0 (1B), −20.3 (1B), −22.9 (1B); ^{31}P {^{1}H} NMR ($CDCl_3$): 35.5 (d, J_{Rh-P} = 149 Hz); ^{13}C {^{1}H} NMR ($CDCl_3$): δ = 10.3 (Cp*−**C**H$_3$), 42.6 (cage−**C**), 95.7 (d, J_{Rh-C} = 7.5 Hz, Cp*), 128.4 (Ph−**C**H), 130.4 (Ph−**C**H), 133.9 (Ph−**C**H), 134.5 (Ph−**C**), 187.3 (dd, $^1J_{Rh-C}$ = 75 Hz, $^2J_{P-C}$ = 10.5 Hz, **C**O) ESI-MS (positive ion mode) *m/z*: 882.33 ([M+K]$^+$, 100%). IR(KBr): ν (cm^{-1}) 2549 (B−H), 1970 (C≡O), 3484 (O−H). Anal. Calcd for $C_{31}H_{40}B_9PS_2Rh_2O_2$: C, 44.17; H, 4.78. Found: C, 43.82; H, 4.62.

3. Monitoring the thermolysis of complex 4 in $CDCl_3$ at 60 ºC by NMR and HRMS

A $CDCl_3$ (0.5 ml) solution of complex **4** in a NMR tube (11 mg, 0.01 mmol) was degassed by pump−freeze−thaw and then heated at 60 ºC for 24 h under argon, and the reaction mixture was monitored by ^{1}H, ^{11}B, ^{31}P NMR and ESI-HRMS measurements. As shown in Fig. S13−S15, complex **4** was decreasing and complex **11** was increasing accompanied by the formation and disappearance of a new species (**10**) containing a Rh−H−Rh bond. The structure of intermediate **10** was proposed in Scheme S2 based on NMR data and ESI-HRMS (positive ion mode, *m/z*: 834.1004

([M+H$^+$]$^+$, see Fig. S16). The short life of **10** precluded additional characterization. Heating for 24 h led to the complete conversion of **4** to **11**. Additionally, in the first 2 h, another more short-lived intermediate with a Rh−H−B bond (a broad signal at −3.69 ppm for the hydride), proposed as **B** in Scheme S2, was observed from these ^{1}H and ^{31}P NMR spectra (see Fig. 13 and 15).

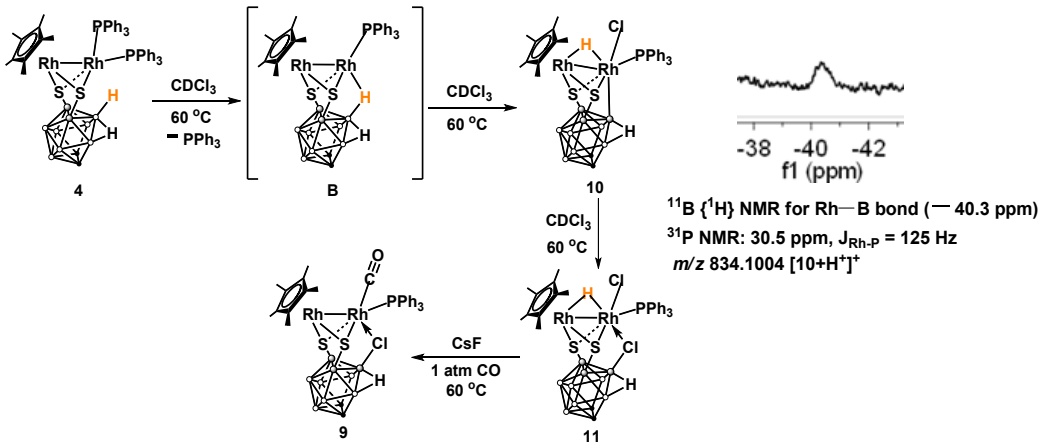

Scheme S2. The conversion of complex **4** in $CDCl_3$ at 60 ºC.

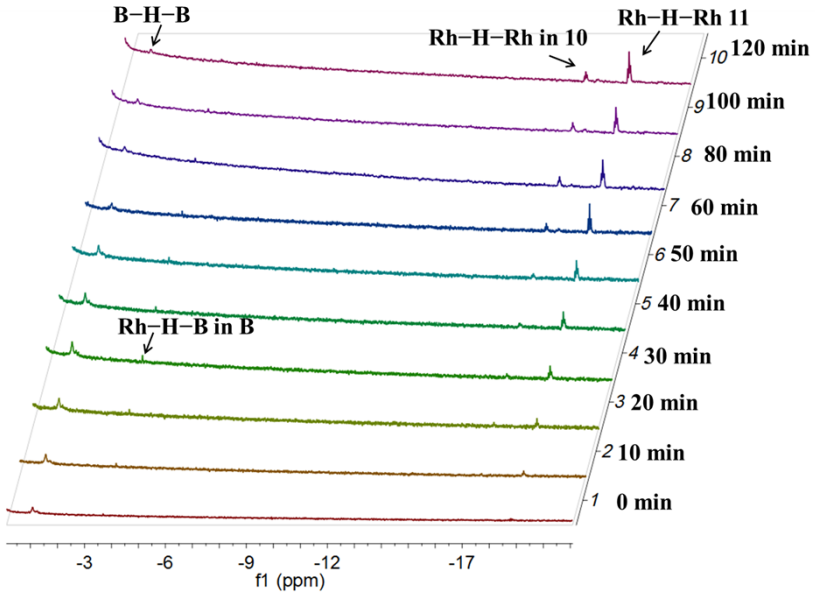

Fig. S13 Monitoring the thermolysis of complex **4** at 60 ºC by ^{1}H {^{11}B} NMR in $CDCl_3$ from 0 to 2 h. Complex **10** was increasing during this stage along with the formation of complex **11**. Rh−H−B resonance was also observed at δ = −3.69 ppm for

the very early intermediate **B** in Scheme S2, indicating B−H is being activated by Rh.

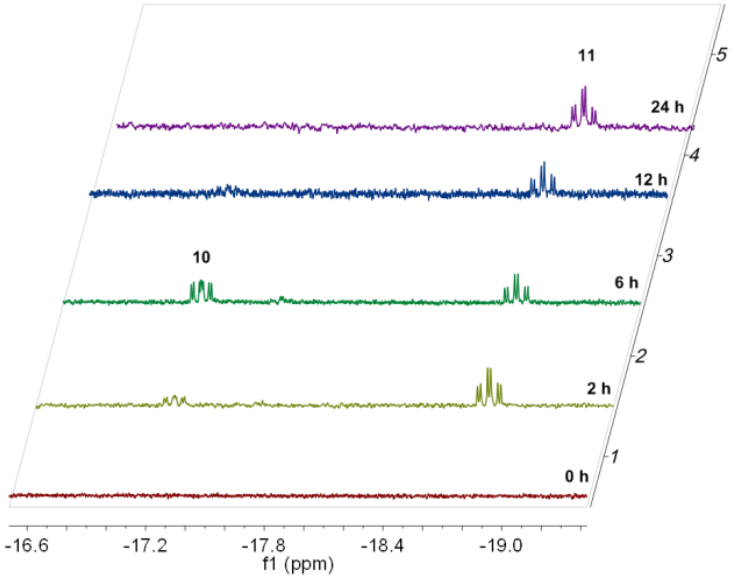

Fig. S14 Monitoring the thermolysis of complex **4** at 60 °C by ^{1}H NMR in $CDCl_3$ showing the conversion from **10** to **11** through B−Cl reductive elimination.

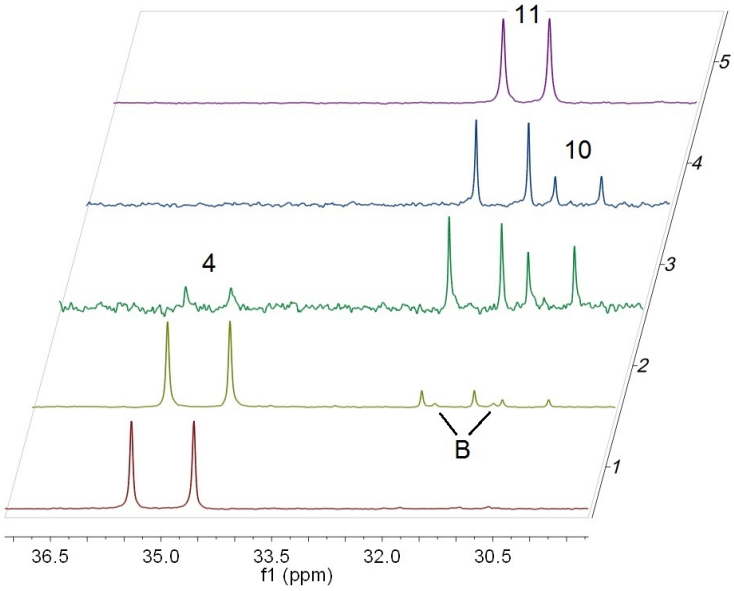

Fig. S15 Monitoring the thermolysis of complex **4** at 60 °C by ^{31}P NMR in $CDCl_3$ to show the conversion from **10** to **11**. The new species observed at 2 h corresponds to the proposed intermediate **B** in Scheme S2.

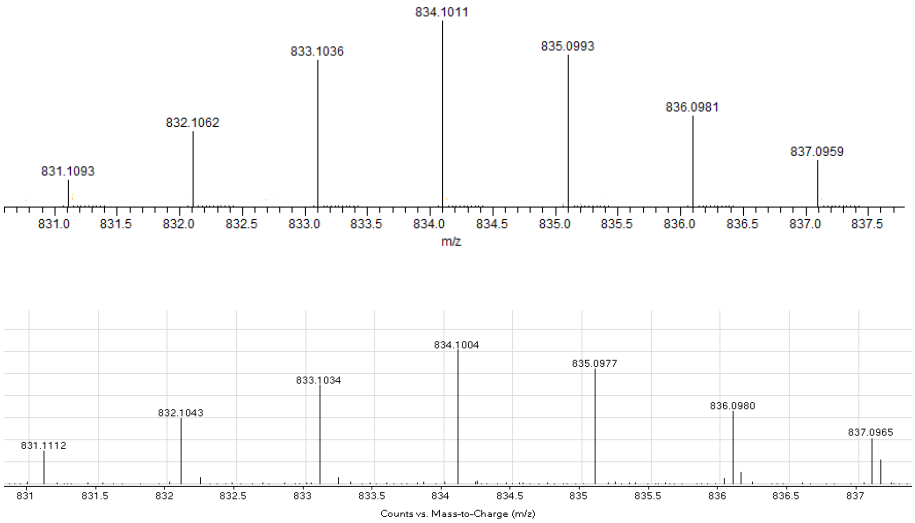

Fig. S16 Monitoring the thermolysis of complex **4** at 60 °C. This measurement was conducted at 6 hours by ESI-HRMS for detecting intermediate **10**. Measured for $[M+H^+]^+$ = 834.1004 (down) and calculated for $[M+H^+]^+$ = 834.1011, M = $C_{30}H_{39}B_9PS_2ClRh_2$ (up).

4. Monitoring the reaction of complex 4 and H_2O in toluene-d_8 by NMR and HRMS

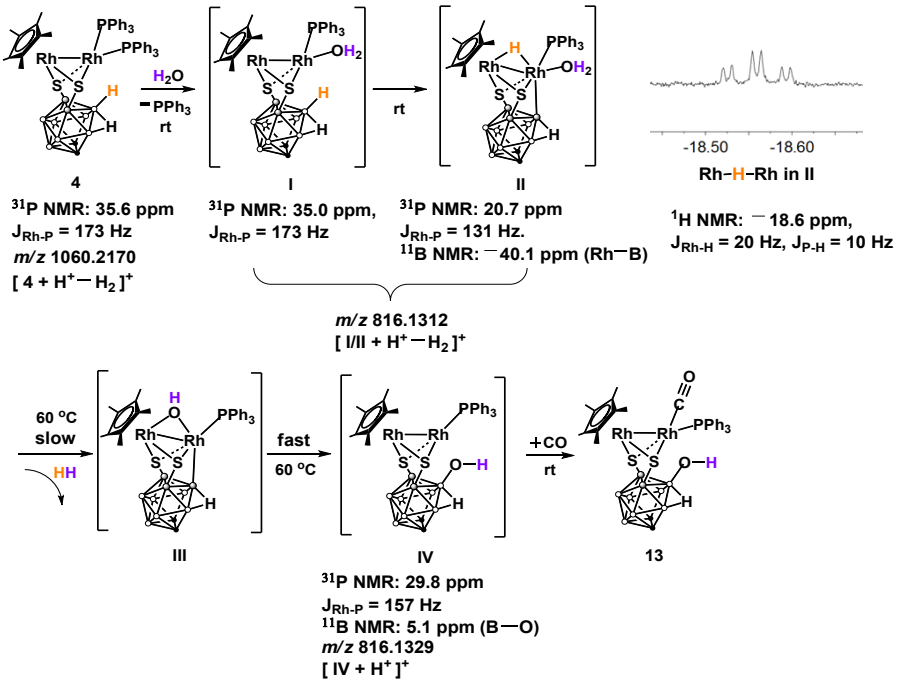

Scheme S3. Proposed mechanism for the formation of B−O bond in the reaction of **4** and water.

A toluene-d_8 (0.5 ml) solution of complex **4** in a NMR tube (11 mg, 0.01 mmol) was added with H_2O (5 μL). Then the mixture was degassed twice by pump−freeze−thaw. After getting to room temperature, the mixture was measured by ^{1}H, ^{11}B, ^{31}P NMR and ESI-HRMS. The ^{31}P NMR indicated the easy PPh_3 ligand dissociation in the presence of water as $O{=}PPh_3$ was observed. Accordingly, a new Rh−P species at 35.0 ppm for ^{31}P (Fig. S17) was observed which is close to the signal at 35.6 ppm in **4**. Its ^{11}B NMR data is also close to that of **4**, only a little upfield shifted (Fig. S17). If the solution in the NMR tube was vigorously shaken at room temperature, the ^{11}B $\{^{1}H\}$ NMR exhibited another new Rh−B resonance at −40.1 ppm (Fig. S17) and the ^{1}H NMR exhibited the typical Rh−H−Rh hydride signal as a triplet centered at −18.6 ppm (Scheme S3), demonstrating the easy B−H activation by Rh when the steric hindrance from bulky PPh_3 is released. The ^{31}P NMR showed a new double peak at 20.7 ppm, thus we propose this species as intermediate **II** which is relatively stable. Correspondingly, at this stage by ESI-HRMS measurement we observed *m/z* = 816.1312 for [**I** or **II** $+H^{+}-H_2]^{+}$, demonstrating the presence of the coordinative H_2O. Water coordination to rhodium center as a weak ligand has been previously reported.[S5] Also, the peak at 798.1207 was observed to assign to [**I** or **II**$+H^{+}-H_2O-H_2]^{+}$ or [**4**$+H^{+}-PPh_3-H_2]^{+}$ (see Fig. S18). Note that loss of H_2 in the MS measurements for different carboranes have been previously reported.[S2a,b] All these evidences support intermediates **I** and **II** and water coordination to dirhodium at the early stage of this reaction.

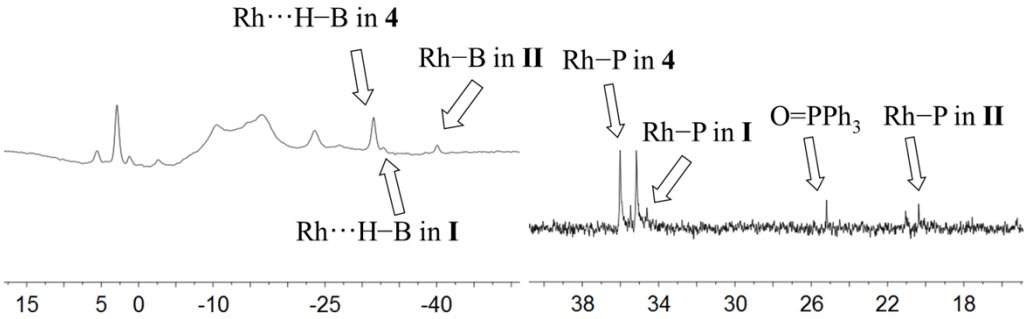

Fig. S17 ^{11}B {^{1}H} and ^{31}P NMR spectra for the mixture of **4** and H_2O, indicating that bulky ligand dissociation and B–H activation have occurred at room temperature.

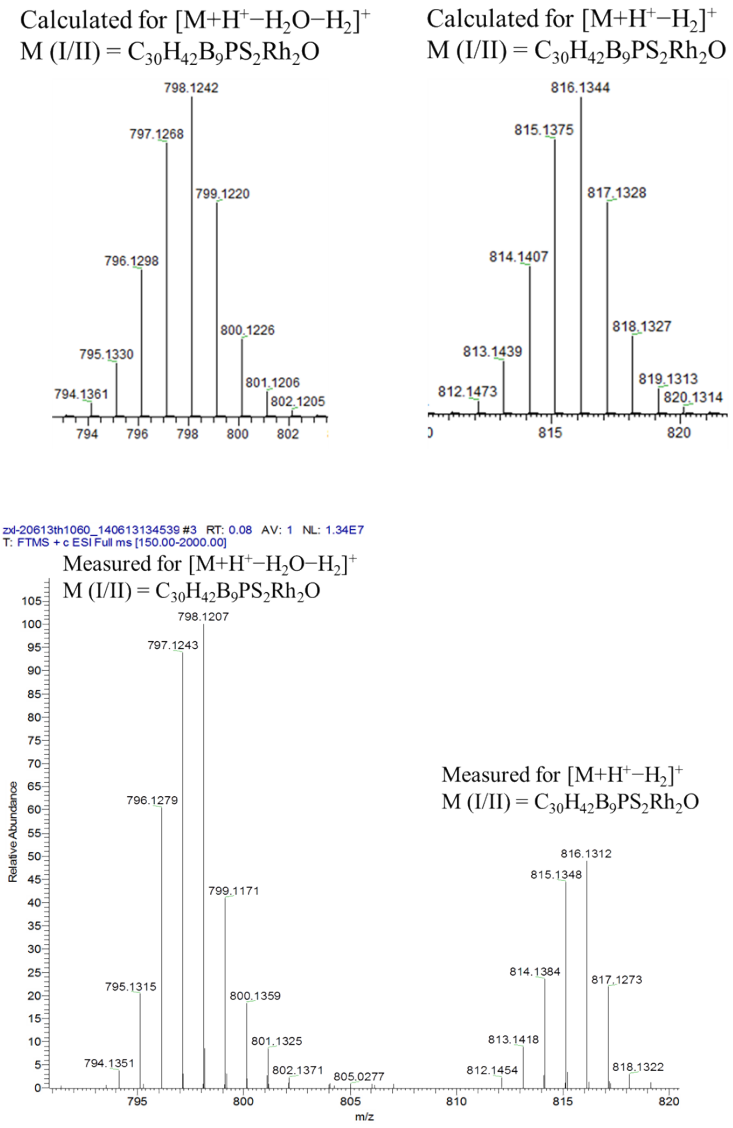

Fig. S18 Using ESI-HRMS to trap intermediates **I** and **II** in the reaction of **4** and water at RT. Two types of molecular ion peaks at 798.1228 and 816.1343 (down, measured) were observed, which are consistent with the calculated molecular ion peaks $[M+H^+-H_2O-H_2]^+$ = 798.1242 and $[M+H^+-H_2]^+$ = 816.1344 (up) for M = $C_{30}H_{42}B_9PS_2Rh_2O$.

Considering the low conversion for the reaction of **4** and water at room temperature, elevated temperature is needed to drive the reaction. The reaction was monitored by ^{31}P NMR at 60 ^oC (Fig. S19). The signal of intermediate **II** quickly disappeared after heating at 60 ^oC. And a new species **IV** was observed as detected by NMR (29.8 ppm for ^{31}P and 5.1 ppm for ^{11}B of the B−O formation). The ESI-HRMS showed the ion peak at 816.1329 for $[M+H^+]^+$ (in comparison to calculated $[M+H]^+$ = 816.1345 for M = $C_{30}H_{40}B_9PS_2Rh_2O$ (Fig. S20)). At the late stage of the reaction, intermediate **IV** was observed as the only new species which is stable. Intermediate **III** was not observed by NMR probably owing to the fast reductive elimination of OH to form thermodynamically favored B−O bond at a higher temperature. After heating at 60 ^oC for 30 h, CO bubbling into the reaction mixture led to complex **13** (>80% yield). This experiment indicates that complex **4** can readily react with water by PPh_3 dissociation, followed by B−H oxidative addition at dirhodium centers and B−O formation to generate thermodynamically stable species.

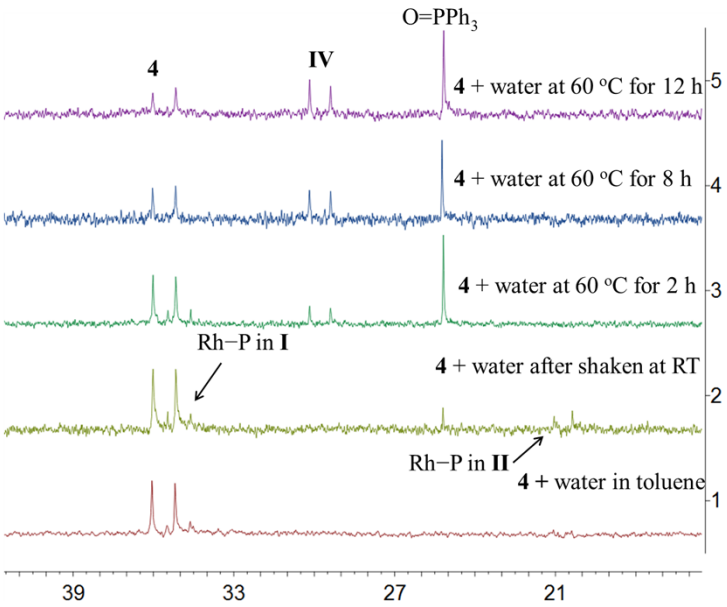

Fig. S19 Monitoring the reaction of complex **4** and water by ^{31}P NMR at room temperature and 60 °C in toluene-d_8.

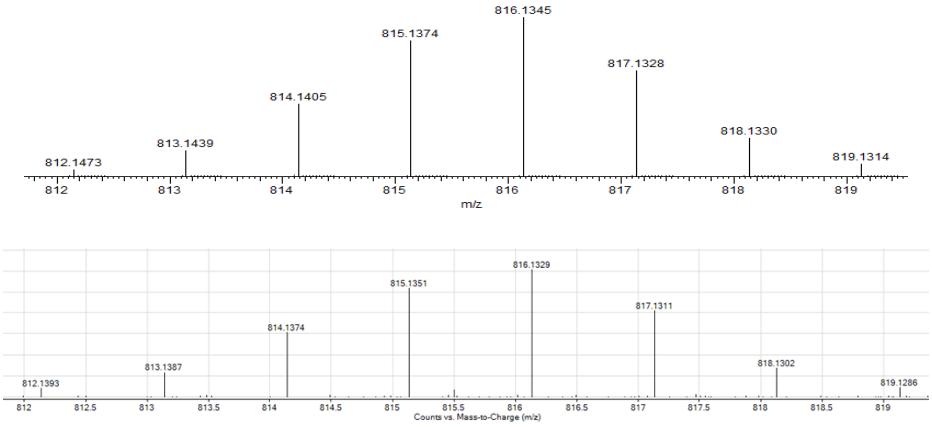

Fig. S20 Using ESI-HRMS to trap intermediate **IV** in the reaction of **4** and water at 60 °C. Measured $[M+H]^+$ = 816.1329 for intermediate **IV** (down) and calculated ($[M+H]^+$ = 816.1346 for M = $C_{30}H_{40}B_9PS_2Rh_2O$) (up).

Table S1. Monitoring the reaction of complex **4** and water. Accurate mass measurements by ESI-HRMS[a]

Complex/Intermediate	Formula	Measured value	Calculated mass (*m/z*)	Ion assignment	mmu[b]	Accuracy (ppm)[c]
4	$C_{48}H_{55}B_9P_2S_2Rh_2$	1060.2170 (p)[d]	1060.2175	$[M+H^+-H_2]^+$	−0.5	−0.5
		798.1207 (p)	798.1242	$[M+H^+-H_2-PPh_3]^+$	−3.5	−4.4
		1060.2173 (n)[d]	1060.2175	$[M-H^+]^-$	−0.2	−0.2
I/II	$C_{30}H_{42}B_9PS_2Rh_2O$	798.1207 (p)	798.1242	$[M+H^+-H_2O-H_2]^+$	−3.5	−4.4
		816.1312 (p)	816.1344	$[M+H^+-H_2]^+$	−3.2	−3.9
IV	$C_{30}H_{40}B_9PS_2Rh_2O$	816.1325 (p)	816.1345	$[M+H^+]^+$	2.0	2.4

[a] See experimental conditions described in general procedure.
[b] Mass error in millimass units.
[c] Accuracy expressed in terms of parts per million (ppm), ppm = 10^6 $\Delta m/m$, where Δm is the difference between the observed and calculated mass.
[d] (p): measured in positive ion mode. (n) measured in negative ion mode.

5. Hydrogen gas (H_2) detection in the reaction of 4 with H_2O in toluene

Compound **4** (159 mg, 0.2 mmol), 0.1 mL of water (25 equiv) and 20 mL toluene was added in an autoclave. Then the autoclave was purged with argon for 3 times and closed under argon (6 atm). The mixture was heated at 60 ºC for 18 h and then the gas phase was tested by GC equipped with a thermal conductivity detector. Argon was used as the GC carrier gas. As a result, H_2 was clearly observed and the result could be repeated in parallel tests (Fig. S21). Detection of H_2 supports the intermolecular dehydrogenation pathway caused by activating O−H of water and B−H bond of carborane. However, both bonds are inert, thus activation of such bonds at dirodium centers under mild conditions are interesting. (Note that bubbling CO into the reaction mixture led to complex **13** over 80%).

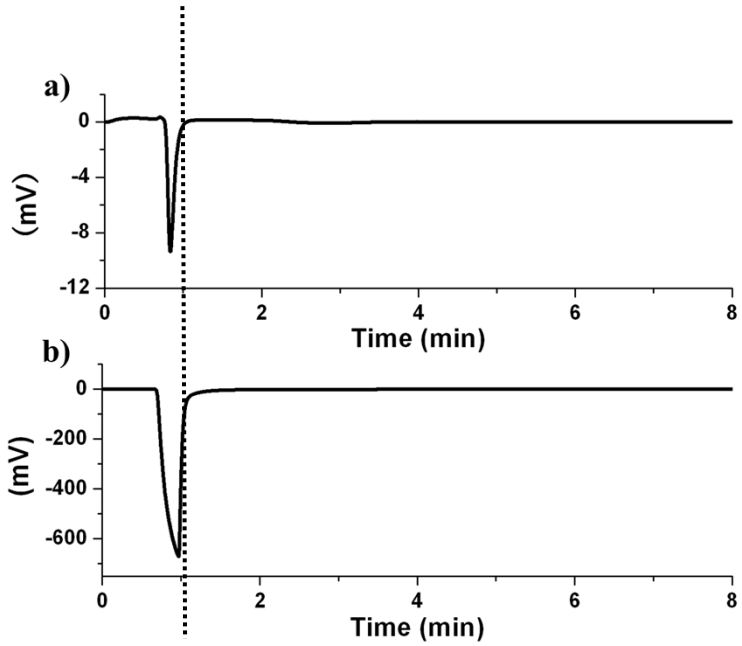

Fig. S21 Testing conditions: HuaAi GC 9560 with TCD; 5 Å molecular sieve column (3 mm × 4 m); carrier gas; argon (20 Ml/min); column temperature: 40 °C; TCD temperature: 120 °C; bridge current: 60 Ma. (a) reaction of complex **4** and H_2O in toluene; (b) H_2 control.

In conclusion, based on the above experimental details, a plausible mechanism for the reaction of **4** and water (or CH_3OH) has been proposed, as shown in Scheme S3. The process starts from PPh_3 ligand dissociation to initiate B−H bond oxidative addition, then dehydrogenation and B−O bond reductive elimination follow up. Detection of the bridging rhodium hydride and Rh−B bond support the B−H bond oxidative addition. Detection of H_2 and isolation of complexes **12** and **13** containing B−O bond support the dehydrogenation and B−O reductive elimination pathway.

6. Crystal data

Table S2. Crystallographic data of compounds **2**−**5**, **7**−**9** and **11**−**13.**

	2	**3**	**4**
Empirical	$C_{12}H_{25}B_{10}S_2Rh$	$C_{48}H_{55}B_{10}F_6P_3S_2Rh_2$	$C_{48}H_{55}B_9P_2S_2Rh_2$
Formula wt	444.45	1216.87	1061.09
Crystal system	Orthorhombic	Monoclinic	Monoclinic
Space group	Pbca	P21/c	P2(1)/n
a/ Å	11.7502(18)	25.340(3)	10.4232(13)
b/ Å	12.940(2)	20.953(2)	22.0424(19)
c/ Å	26.299(4)	22.865(2)	25.4131(17)
α/deg	90	90	90
β/deg	90	93.648(3)	91.218(3)
γ/deg	90	90	90
V/ Å^3	3998.7(11)	12116(2)	5837.4(10)
Z	8	8	4
ρ_{calcd} (g cm^{-3})	1.477	1.334	1.207
abs coeff (mm^{-1})	1.055	0.742	0.720
F(000)	1792	4912	2160
θ range (deg)	1.55 /25.99	0.81/26.00	1.22/26.00
no. of rflns collected	28883	71768	34752
no. of indep rflns	3925	23803	11461
no. of obsd rflns (I>2σ(I))	3498	16988	7284
GoF	1.046	1.042	1.046
R1/wR2 (I> 2σ(I))	0.0363/0.1039	0.0521/0.1291	0.0513/0.1359
R1/wR2 (all data)	0.0401/0.1077	0.0590/0.1305	0.0592/0.1367
largest peak/hole (e Å^{-1})	0.882 /−1.953	0.933/−0.785	0.634 /−0.819

	5	**7·(CH$_2$)$_6$**	**8·CH$_2$Cl$_2$**
Empirical	$C_{31}H_{40}B_9PS_2Rh_2O$	$C_{31}H_{39}B_9PS_2Rh_2OCl\cdot(CH_2)_6$	$C_{48}H_{54}B_9P_2S_2ClRh_2\cdot CH_2Cl_2$
Formula wt	826.83	945.43	1180.46
Crystal system	Monoclinic	Monoclinic	Monoclinic
Space group	P2(1)/c	P2(1)/n	P21/c
a/ Å	10.4072(16)	11.8553(8)	10.5802(14)
b/ Å	15.6144(19)	22.2136(15)	11.9277(16)
c/ Å	22.4334(13)	17.9969(12)	40.511(5)
α/deg	90	90	90
β/deg	101.504(3)	93.097(2)	92.389(2)
γ/deg	90	90	90
V/ Å^3	3572.2(7)	4732.5(6)	5107.9(12)
Z	4	4	4
ρ_{calcd} (g cm^{-3})	1.537	1.327	1.535
abs coeff (mm^{-1})	1.112	0.903	0.983
F(000)	1664	1920	2392

θ range (deg)	2.00/27.74	1.46/27.54	1.01/26.00
no. of rflns collected	32187	42547	36040
no. of indep rflns	8354	10887	9633
no. of obsd rflns (I>2σ(I))	6691	8254	7899
GoF	1.066	1.046	1.085
R1/wR2 (I> 2σ(I))	0.0574/0.14460	0.0600/0.1473	0.0533/0.1245
R1/wR2 (all data)	0.0592/0.14490	0.0642/0.1482	0.0607/0.1263
largest peak/hole (e Å^{-1})	0.701/−0.696	0.861/−0.818	0.865/−0.730

	9	**11·CH_2Cl_2**	**12**
Empirical	$C_{31}H_{39}B_9PS_2Rh_2OCl$	$C_{30}H_{40}B_9PS_2Cl_2Rh_2\cdot CH_2Cl_2$	$C_{32}H_{42}B_9PS_2Rh_2O_2$
Formula wt	861.27	954.65	855.86
Crystal system	Monoclinic	Monoclinic	Monoclinic
Space group	P2(1)/c	P2(1)/n	P2(1)/n
a/ Å	10.3532(9)	10.1173(15)	10.6217(15)
b/ Å	15.6988(15)	18.265(3)	22.947(3)
c/ Å	22.680(2)	22.185(3)	15.445(2)
α/deg	90	90	90
β/deg	100.705(2)	100.007(2)	101.289(2)
γ/deg	90	90	90
V/ Å^3	3622.1(6)	4037.3(10)	3691.6(9)
Z	4	4	4
ρ_{calcd} (g cm^{-3})	1.579	1.571	1.540
abs coeff (mm^{-1})	1.171	1.249	1.080
F(000)	1728	1912	1724
θ range (deg)	1.59/27.66	1.86/26.00	1.61/26.00
no. of rflns collected	24205	30917	26294
no. of indep rflns	8418	7918	7222
no. of obsd rflns (I>2σ(I))	5068	6950	5469
GoF	1.002	1.037	0.967
R1/wR2 (I> 2σ(I))	0.0673/0.1406	0.0355/0.0956	0.0711/0.1768
R1/wR2 (all data)	0.0604/0.1416	0.0383/0.0966	0.0838/0.1842
largest peak/hole (e Å^{-1})	0.645/−0.569	0.359/−0.489	1.895/−1.060

	13
Empirical	$C_{31}H_{40}B_9PS_2Rh_2O_2$
Formula wt	842.83
Crystal system	Monoclinic
Space group	P2(1)/c
a/ Å	10.4299(18)
b/ Å	15.6029(16)
c/ Å	22.3267(17)
α/deg	90
β/deg	101.465(2)

γ/deg	90
V/ Å^3	3560.9(8)
Z	4
ρ_{calcd} (g cm^{-3})	1.572
abs coeff (mm^{-1})	1.119
F(000)	1696
θ range (deg)	1.60/26.00
no. of rflns collected	27622
no. of indep rflns	6953
no. of obsd rflns (I>2σ(I))	5651
GoF	1.070
R1/wR2 (I> 2σ(I))	0.0537/0.1343
R1/wR2 (all data)	0.0559/0.1348
largest peak/hole (e Å^{-1})	0.625/−0.595

7. Calculation details

The present calculations were carried out with the Gaussian09 program package.[S6] The geometry of complexes **A**, **2**, **4**, **5, 7, 9** and **11** were optimized based on their X-ray crystal structures by the density functional theory (DFT) without symmetry constraint. Analysis of molecular orbitals were carried out at the B3PW91/6-31G(d, p)/LANL2DZ [Rh] level of theory. The NBO approach was used to calculate the orbital populations, Wiberg bond indices (WBI), natural population analysis (NPA) and second-order perturbation analysis.

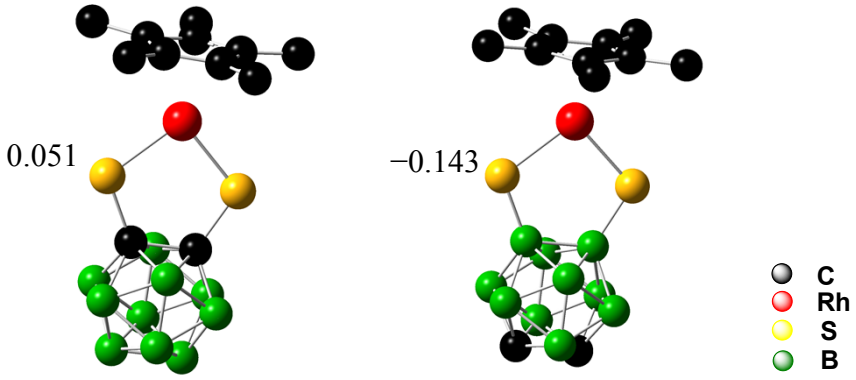

Fig. S22 Optimized structures of **A** and **2**.

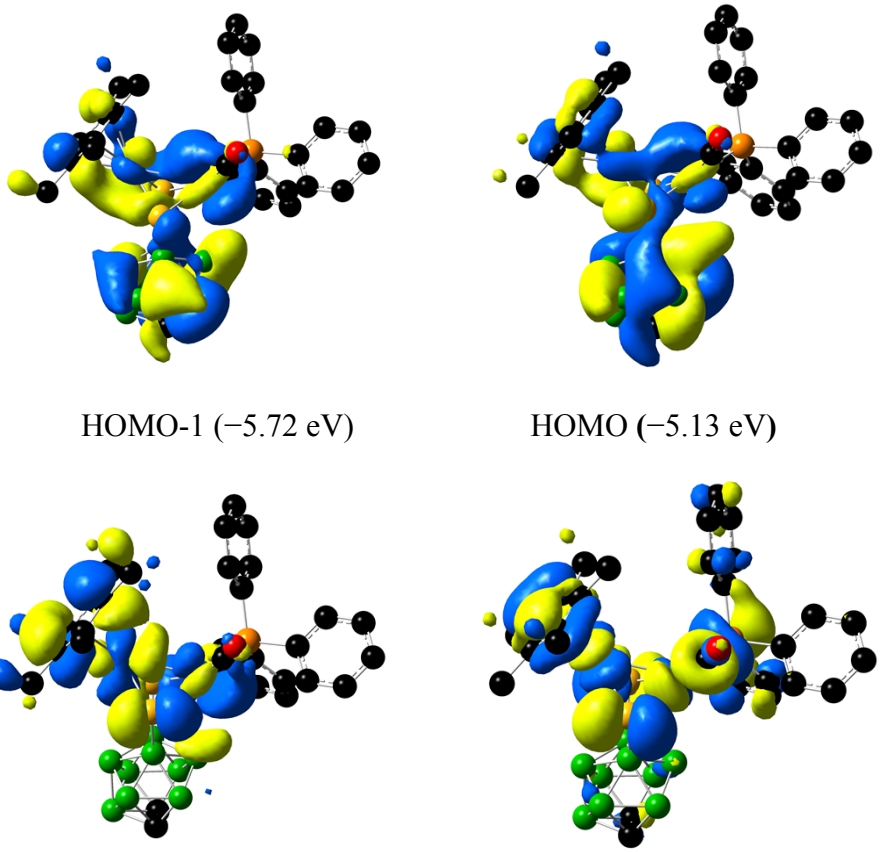

HOMO-1 (−5.72 eV) HOMO (−5.13 eV)

LUMO (−2.59 eV) LUMO+1 (−1.76 eV)

Fig. S23 Molecular orbitals for complex **5**.

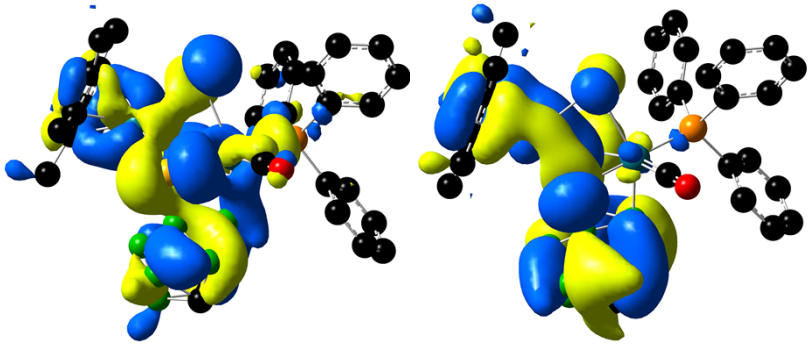

HOMO-1 (−5.77 eV) HOMO (−5.56 eV)

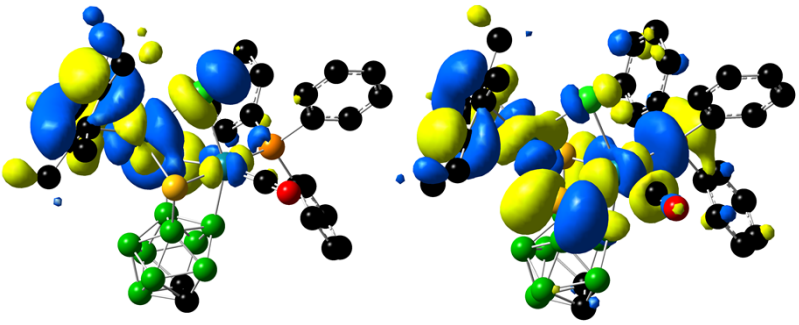

LUMO (−2.02 eV) LUMO+1 (−1.89 eV)

Fig. S24 Molecular orbitals for complex **7**.

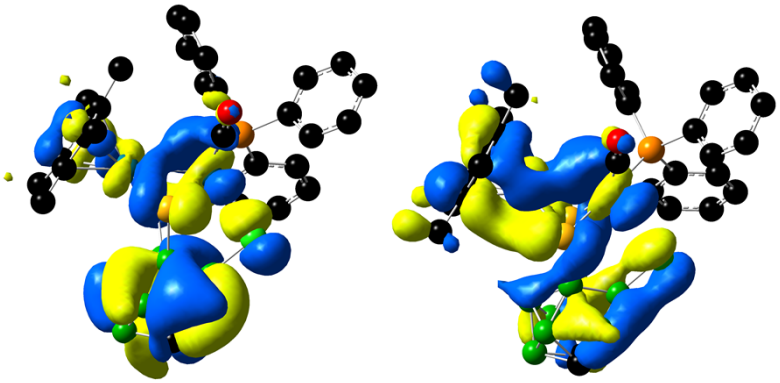

HOMO-1 (−5.56 eV) HOMO (−5.50 eV)

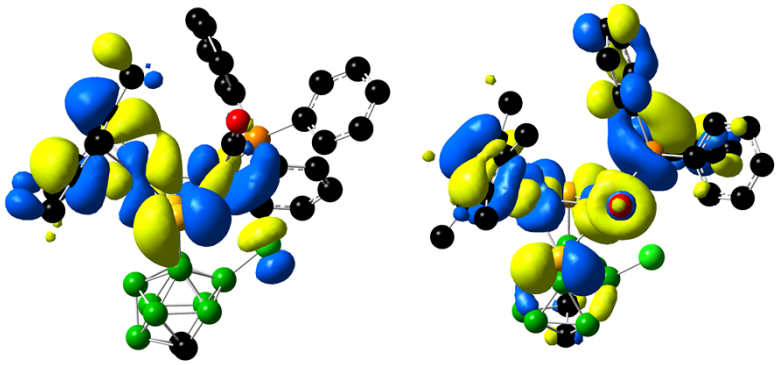

LUMO (−2.51 eV) LUMO+1 (−1.82 eV)

Fig. S25 Molecular orbitals for complex **9**.

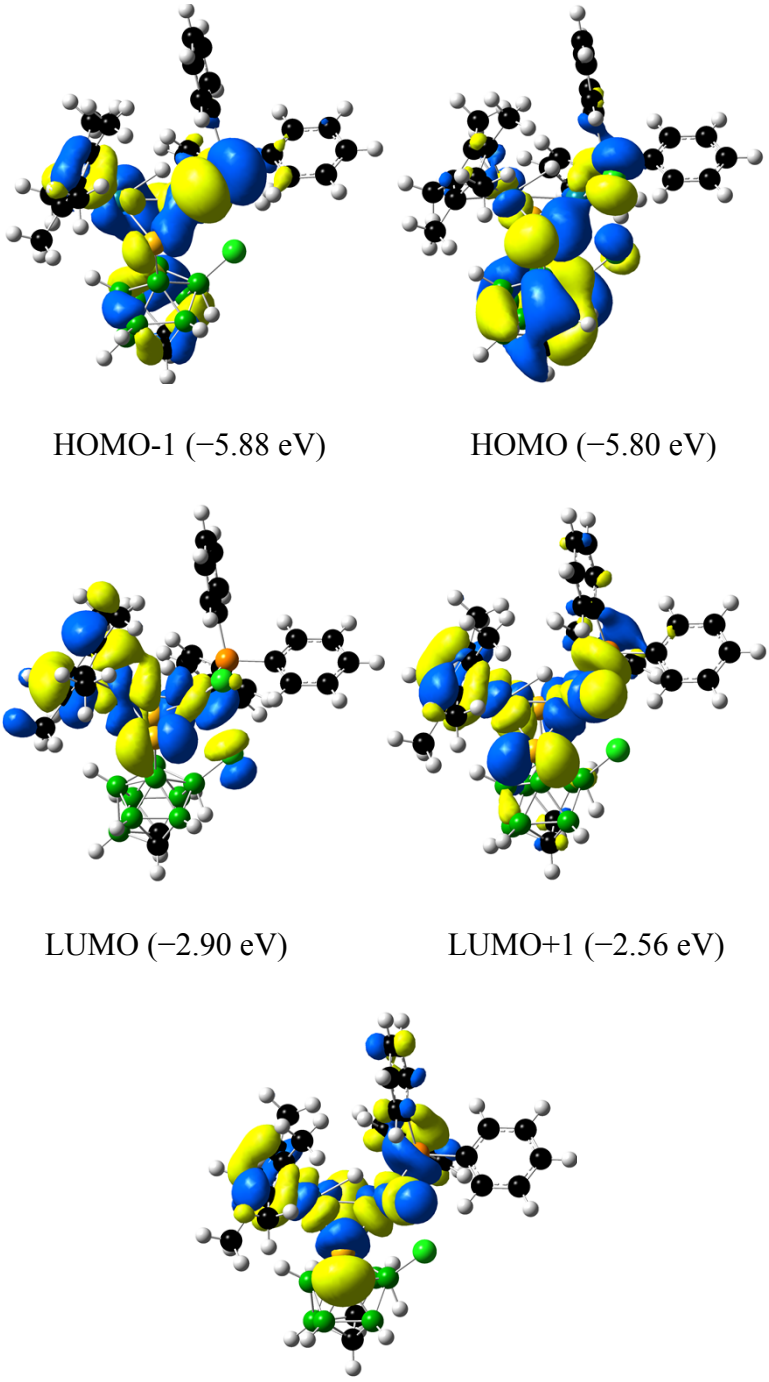

Fig. S26 Molecular orbitals for complex **11**.

8. References

(S1) J. Plešek, Z. Janoušek, S. Heřmánek, *Coll. Czech. Chem. Comm.* 1980, **45**, 1775.

(S2) (a) T. R. I. Cataldi, G. Ricciardi, G. Bianco, D. Pietrangeli, S. Abate, *Rapid*

Commun. Mass Spectrom. 2009, **23**, 1927. (b) C. L. Brown, K. P. Gross, T. Onak, *J. Am. Chem. Soc.* 1972, **94**, 8055. (c) I. Slepukhina, T. Duelcks, H. M. Schiebel, D. Gabel, *J. Organomet. Chem.* 2005, **690**, 2796. (d) C. Viñas, A. Larrmanine, F. Teixidor, H. Horáková, A. Langauf, R. Vespalec, I. Mataa, E. Molins, *Dalton Trans.* 2007, 3369. (e) G. Barberà, C. Viñas, F. Teixidor, A. J. Welch, G. M. Rosair, *J. Organomet. Chem.* 2002, **657**, 217.

(S3) G. M. Sheldrick, SADABS, *A Program for Empirical Absorption Correction*; University of Göttingen; Göttingen, Germany, **1998**.

(S4) G. M. Sheldrick, SHELXL-97, *Program for the Refinement of Crystal Structures*; University of Göttingen; Göttingen, Germany, **1997**.

(S5) (a) D. P. Smith, H. Chen, S. Ogo, A. I. Elduque, M. Eisenstein, M. M. Olmstead, R. H. Fish, *Organometallics* 2014**, 33**, 2389. (b) X. F. Fu, S. Li, B. B. Wayland, *J. Am. Chem. Soc.* 2006, **128**, 8947.

(S6) M. J. Frisch, G. W. Trucks, H. B. Schlegel, G. E. Scuseria, M. A. Robb, J. R. Cheeseman, Jr., J. A. Montgomery, T. Vreven, K. N. Kudin, J. C. Burant, J. M. Millam, S. S. Iyengar, J. Tomasi, V. Barone, B. Mennucci, M. Cossi, G. Scalmani, N. Rega, G. A. Petersson, H. Nakatsuji, M. Hada, M. Ehara, K. Toyota, R. Fukuda, J. Hasegawa, M. Ishida, T. Nakajima, Y. Honda, O. Kitao, H. Nakai, M. Klene, X. Li, J. E. Knox, H. P. Hratchian, J. B. Cross, C. Adamo, J. Jaramillo, R. Gomperts, R. E. Stratmann, O. Yazyev, A. J. Austin, R. Cammi, C. Pomelli, J. W. Ochterski, P. Y. Ayala, K. Morokuma, G. A. Voth, P. Salvador, J. J. Dannenberg, V. G. Zakrzewski, S. Dapprich, A. D. Daniels, M. C. Strain, O. Farkas, D. K. Malick, A. D. Rabuck, K. Raghavachari, J. B. Foresman, J. V. Ortiz, Q. Cui, A. G. Baboul, S. Clifford, J. Cioslowski, B. B. Stefanov, G. Liu, A. Liashenko, P. Piskorz, I. Komaromi, R. L. Martin, D. J. Fox, T. Keith, M. A. Al-Laham, C. Y. Peng, A. Nanayakkara, M. Challacombe, P. M. W. Gill, B. Johnson, W. Chen, M. W.Wong, C. Gonzalez, J. A. Pople, Gaussian 03, Revision C.02 and Revision D.02, Gaussian, Inc., Wallingford CT, 2004.